University of Baghdad
College of Engineering
JE
JOURNAL OF ENGINEERING

Journal of Engineering

journal homepage: www.jcoeng.edu.iq

Volume 30 Number 4 April 2024

Experimental Investigation of Forced Convection in Plain or Partly Inserted Square Channel with Porous Media

Sarmad A. Ali [1,*], Suhad A. Rasheed [2]
Department of Mechanical Engineering, University of Technology, Baghdad, Iraq
me.21.06@grad.uotechnology.edu.iq[1], suhad.a.aljumaily@uotechnology.edu.iq[2]

ABSTRACT

Several techniques are used to improve the channels' heat transfer coefficient and Nusselt number. One of the methods used for these improvements is porous media (PM). This research deals with an experimental study of heat transfer by forced convection inside a square-shaped channel (0.12 x 0.12 m^2) with a length of (0.5 m) and a hydraulic diameter of (0.12 m). The heat flux (4791.7 W/m^2) is exposed below the test section, and other walls are thermally insulated. The air was used as the working fluid for the Reynolds number range (2689.6 to 5806.3). The channel was partially filled with the PM (glass spheres with 5mm diameter) by taking three different heights layers (20, 40, and 60 mm) and knowing its effect on the temperature distribution, the local heat transfer coefficient, locally Nusselt number, and the average heat transfer coefficient and Nusselt number. Also, the same parameters were studied without PM inside the channel (plain). The results showed that the PM improved the heat transfer coefficient and the Nusselt number. Also, the temperature distribution decreased gradually with the Reynolds number increase for each height layer, the local heat transfer coefficient and local Nusselt number gradually reduced with the length of the test section increase for each Reynolds number, average Nusselt number increased gradually with the growth of the Reynolds number for each height layer. The PM layer at a height of (60 mm) gave the best improvement in the heat transfer coefficient and Nusselt number compared to the other layers. In addition, the friction factor across the test section at this layer decreases gradually with increasing fluid velocity.

Keywords: Forced convection, Heat transfer, Partially filled, Porous medium, Square channel, Glass spheres.

*Corresponding author
Peer review under the responsibility of University of Baghdad.
https://doi.org/10.31026/j.eng.2024.04.07

Article received: 11/05/2023
Article accepted: 27/07/2023
Article published: 01/04/2024

التحقيق التجريبي للحمل القسري في قناة مربعة فارغة أو مدرجة جزئيًا بوسائط مسامية

سرمد احمد علي* ، سهاد عبد الحميد رشيد

قسم الهندسة الميكانيكية، الجامعة التكنولوجية، بغداد، العراق

الخلاصة

تستخدم العديد من التقنيات لتحسين معامل انتقال الحرارة وعدد نسلت في القنوات، إحدى هذه الطرق هي الوسائط المسامية. يتناول هذا البحث دراسة عملية لانتقال الحرارة بالحمل القسري داخل قناة ذات مقطع عرضي مربع الشكل (0.12 x 0.12 م^2) بطول (0.5 م) وقطرهيدروليكي (0.12 م). تم تسليط الفيض الحراري (4791.7 واط / م^2) أسفل قسم الاختبار وتم عزل الجدران الأخرى حرارياً، تم استخدام الهواء كمائع عامل لهذه الظاهرة ولمدى لعدد رينولدز (5806.3 to 2689.6)، وتم ملء القناة جزئيًا بالمادة المسامية (كرات زجاجية بقطر 5 ملم) بأخذ ثلاث طبقات بارتفاعات مختلفة (20 ، 40 ، 60 ملم) ومعرفة تأثيرها على توزيع درجات الحرارة ، معامل انتقال الحرارة الموقعي ، عدد نسلت الموقعي ، متوسط عدد نسلت ، ومقارنة النتائج دون وجود هذه الكرات داخل مقطع الاختبار للقناة. أظهرت نتائج هذه الدراسة أن المادة المسامية تحسّن وتعزز من معامل انتقال الحرارة وعدد نسلت. بالإضافة إلى ذلك انخفض توزيع درجات الحرارة تدريجيًا مع زيادة عدد رينولدز لكل طبقة ارتفاع وانخفض معامل انتقال الحرارة الموقعي وعدد نسلت الموقعي تدريجيًا مع زيادة طول قسم الاختبار لمحور الجريان لكل عدد رينولدز، وزاد متوسط عدد نسلت تدريجيًا مع الزيادة من عدد رينولدز لكل طبقة ارتفاع. أعطت طبقة الوسط المسامي بارتفاع (60 ملم) أفضل تعزيز وتحسين في معامل انتقال الحرارة وعدد نسلت مقارنة مع طبقات الوسط المسامي الاخرى، إضافة" الى التناقص التدريجي لمعامل الاحتكاك عبر مقطع الاختبار عند هذه الطبقة بزيادة سرعة المائع.

الكلمات المفتاحية: انتقال الحرارة ، الحمل القسري ، قناة مربعة ، وسط مسامي ، كرات زجاجية.

1. INTRODUCTION

Forced convection is created when fluid is forced over the surface of a wall using an internal or external device, such as a revolving cylinder or driven lid, or an external device, such as a fan or compressor. Many techniques are used in engineering applications such as (Heat exchangers, gas transmission pipelines in gas power plants, air conditioning systems, cooling in electronic equipment, solar energy systems, etc.) to improve the heat transfer coefficient and Nusselt number. So, improvements in the heat transfer process result in energy savings by cutting down on running time and construction costs by downsizing machinery. One of these techniques is using a PM of many densely packed particles with fluid-filled holes (voids) inside the channels to gain heat and thus increase the heat transfer coefficient and the Nusselt number **(Mohammed, 2020)**. Also, using a different type of metal foam as a PM, including closed and open cells enhances the performance and thermal system in these applications **(Ali, 2015)**. Many researchers **(Poulikakos and Renken, 1987; Dawood and Hmood, 2006; Varol et al., 2008; Abood, 2011; Antonio et al., 2013; Li and Hu, 2019)** studied numerically and experimentally forced convection heat transfer inside the channels

in different (shapes, boundary conditions, porosity, and working fluid) by using various types of PM such as [metal foam, wire mesh, glass spheres, and steel spheres] to enhance the heat transfer coefficient and Nusselt number thus increase the efficiency of thermal and industrial applications. The researcher **(Makkawi, 1995)** conducted a practical study of heat transfer by forcing convection inside a rectangular PM channel and using air as a working fluid. The results showed that the Nusselt number increases with the increase in the Reynolds number.

(Hilal et al., 2012) illustrated an experimental study of heating transfer and pressure drop by forced convection inside a square-shaped channel filled with PM. Air was used as a working fluid. This study showed that the Nusselt number increases with the increase in the Reynold number. The results were compared, and the Nusselt number of the channel was times higher than (1.2 and 1.19) without the presence of the PM. **(Seki et al., 1978)** provided an experimental study of convective heating transport in a constrained rectangular chamber filled with PM, on opposing vertical walls of which various temperatures are forced. Three types of fluids, namely water, transformer oil, and ethyl alcohol, are used to measure each type of solid particle. **(Kurtbas and Celik, 2009)** tested mixed convection (Free and Forced) flow through a horizontal, rectangular channel with open-cell metal foams of varied pore densities (10, 20, and 30 PPI) to determine the heating transfer properties. An equal heat flux was applied at each channel's lateral wall. Temperatures were recorded throughout the whole surface of the walls for each of the uniform heat flux's three possible values. The Reynolds and Richardson numbers are provided as functions of the average and local Nusselt numbers.

(Shokouhmand et al., 2011; Nimvari et al., 2012; Torabi et al., 2015; Nazari and Toghraie, 2017; Kemerli and Kahveci, 2018; Hilal et al., 2014; Li et al., 2019) presented numerical and experimental studies of forced convection heat transfer in channels with different cross-sections, including circular, square and rectangular, through the use of porous media of various types such as saturated wire mesh, metallic, Nano and foam, as a technique to improve the heat transfer process of fluid flow during the test section. The results showed that the presence of the porous material improves the heat transfer coefficient compared to the absence of it inside the test section **(Moghadasi et al., 2020; Khadhrawi et al., 2020; Zhu et al., 2023)**. An experimental study was conducted **(Majel and Obaid, 2024)** to determine water's convective heat transfer coefficient in a flat, micro heat pipe under laminar flow conditions and constant intake temperature. The studies employed different horizontal heat sink temperatures (working temperatures) ranging from 15 to 35°C and a liquid flow rate of 3.563E-8 m3/sec. The heat flux varied between 20 and 50W. The performance of the rectangular microchannel is assessed in terms of temperature profile, heat transfer coefficient, Nusselt number, and thermal resistance. The outcomes show that, provided the heat flow value is not beyond the capillary limitations, the heat resistance progressively falls to its lowest value when the tiny heat pipe temperature gradients are less than those of the copper plate. The results also showed that, for various heat sink temperatures, the coefficient of heat transfer in the condensation zone is lower than in the evaporation zone. A generalised regression equation is created to estimate the Nusselt number for water in a flat micro heat pipe.

(Rasheed and Abood, 2017) presented an experimental study conducted in the forced convection heat transfer of a stable laminar flow of a square duct with dimensions (20 x 20 cm^2) and a length of 40 cm, filled with a saturated PM of the type of glass balls of uniform diameter. An electric heater was placed in the middle of the test section, while the other walls

were thermally insulated. **(Pastore et al., 2018)** performed an experimental study to evaluate the dynamics of forced convection heat transfer due to an electrical pump connected in a thermally insulated column circular pipe with a diameter (11 cm) and height (166 cm) that was filled with a different PM (rock stone) with various size and thermophysical properties. Two different PM forms were utilized using distinct granule sizes and certain surfaces. For local non-thermal equilibrium (LNTE) circumstances, one-dimensional heat. **(Youssif et al., 2020)** carried out experimental tests on forced convective heat transfer for water flowing through a horizontal circular conduit. As a PM, the pipe was filled with two distinct types of particles (steel and a combination of steel and plastic) while being heated at a constant heat flux. Internal, laminar, incompressible, and stable flows with varied heat fluxes of (200, 400, and 600 W/m^2) are the flow characteristics over a wide range of Reynolds numbers (500, 1000, and 1500) in each example, three times for each number. In addition to additional diagrams that illustrate the relationship between the local and average Nusselt number with the data described above, the study's results are shown in terms of temperature distribution to demonstrate temperature behaviors in the pipe. The results for each PM type reveal that for steel and mixed PM, respectively, the local and average Nusselt numbers rise along with the Reynolds numbers. Air mist flow was experimentally investigated in a tube equipped with a PM. The porous area under study has a unique shape. The analysis is also done on the impact of operational parameters like the Reynolds number. The findings show that the presence of PM causes the heat flux applied to the channel walls to be transferred into the fluid due to the PM high conductivity and creation of a uniform space **(Baragh et al., 2019)**. The results also showed that mist cooling in PM can speed up heat transfer as compared to single-phase cooling. Results indicate that combining these two techniques, PM and mist flow, significantly improves heat transfer. **(Guo et al., 2020)** experimental study to explore the velocity distribution of high Reynolds number turbulence above and in PM. This study builds a visual flume test bench to replicate PM as an aggregation of spherical glass beads with a 10 mm diameter. Ultrasonic Doppler velocimetry determines the free flow velocity of fluid passing through the PM and the velocity inside the PM. The slip velocity and momentum transfer close to the interface are explored with the impacts of Reynolds number, relative water depth, and porosity factors. According to the findings, the slip coefficient for a PM bed with a porosity of 0.331 varies from 0.000 082 to 0.000 594, while that of a PM bed with a porosity of 0.476 ranges from 0.000 034 to 0.001 068.

The current study aims to experimentally investigate the effect of PM on the enhancement of forced convective heat transfer impacted by an air blower connected to the channel of the test section partially filled with PM (glass spheres 5 mm diameter). Some of the geometrical and conditional operation parameters are studied, such as the effect of PM height layer (plain, 20, 40, and 60 mm), Reynolds number range of (2689.6 to 5806.3), and constant heat flux at a lower surface of the test section (4791.7 W/m^2).

2. EQUIPMENT FOR EXPERIMENTATION

An experimental setup shown in **Figs. 1 and 2** were created and used in this work. Most of these components were meticulously designed to prevent air leakage during operation and fastening between the linked portions. The square cross-section (H of 0.12m, W of 0.12m, and length of 0.5 m) channel of hydraulic diameter of 0.12 m is made of galvanized iron of 0.5 mm thickness. The channel's air supply was connected using a tiny adaptor. The one-

phase motor's output is 150 W, its rotational speed is 3600 rpm, and its discharge pipe size is (50 mm). Four different flow rates may be achieved by employing a regulator and valve to regulate the air input blower. **Figure 3.** shows the details of the electric blower connected to the control valve for the amount of air entering the test section of the square channel. A digital anemometer was placed at the end of the test section, and the air velocity was estimated by obtaining many readings and averaging them.

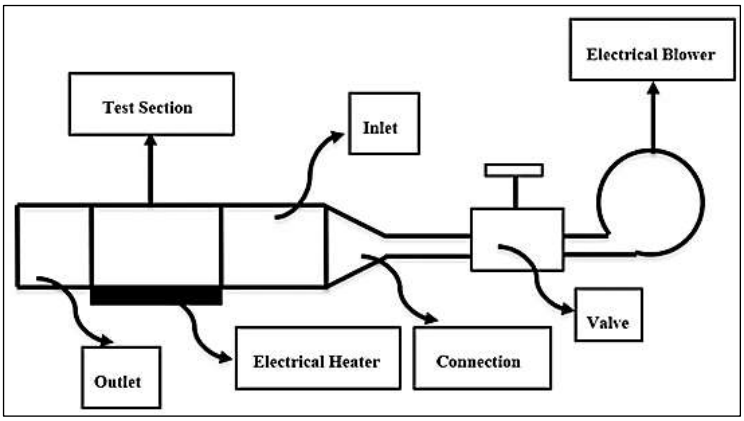

Figure 1. An apparatus schematic for the experimental setup.

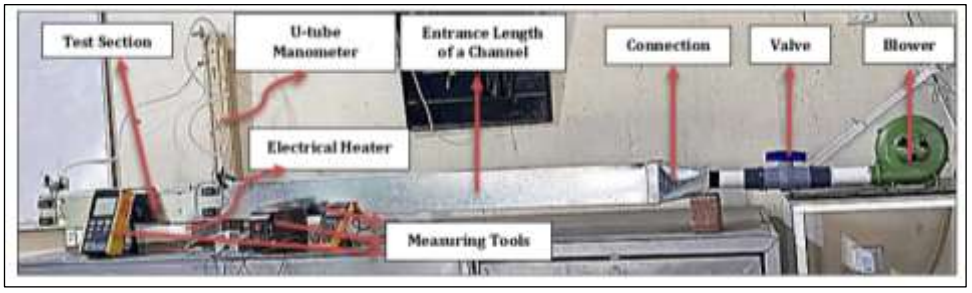

Figure 2. A photograph of the channel with measuring tools.

Ten thermocouples type (K) were positioned across five sections along the surface of the channel to detect the temperature (test section). After that, the fine-grinding paper was used to polish the channel surface properly, as shown in **Fig. 4.**

Figure 3. Electrical blower for a channel.

The insulating material removed all the heater terminals and sensor wires from the test section. Two more sensors were attached at the test section's intake and exit to monitor the air temperature. All the sensors were linked to the temperature recorder device, as shown in **Fig. 2.** The entire test portion was then covered in a layer of thick (70 mm) glass wool to provide excellent insulation outdoors. To ensure no gaps larger than the glass spheres' diameter, especially close to the wall, the channel was randomly partially filled with the objects before being sufficiently shaken. This technique partially filled the test rig's length (0.5m) with the PM. An electrical heater that received AC current from a voltage regulator was used to electrically heat the channel's surface to provide a constant heat flux along the test section. The present processing data are the voltage and current of electrical heaters, measured temperatures using a temperature Lutron type (BTM-4208SD) reader, and the air velocity by a digital anemometer UT363S.

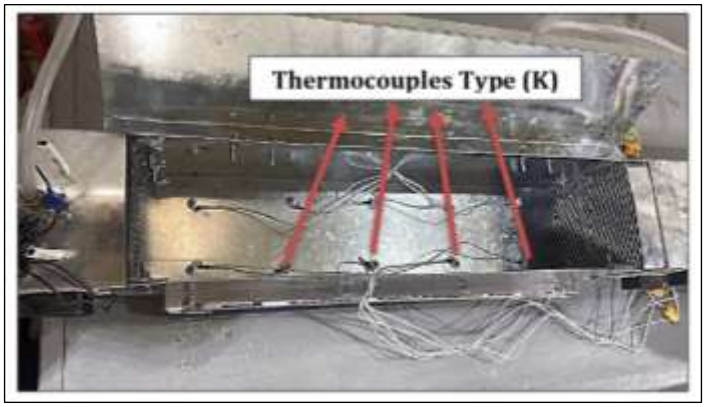

Figure 4. Locations of thermocouples type (K) for a test section.

3. POROUS MEDIA (PM)

In this work, glass spheres with a diameter of (5 mm) were used as a PM, where the test section was partially filled by changing the layers of the PM, as shown in **Fig. 5.**

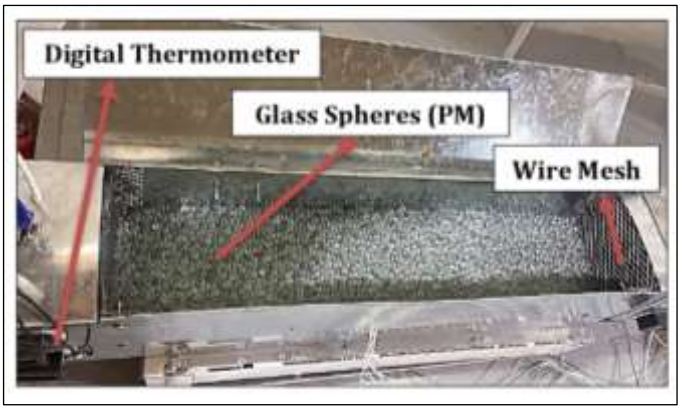

Figure 5. The test section is partially filled with glass spheres used as PM.

Also, the main thermo-physical characteristics of the PM are listed:

- **Porosity of PM**

The porosity of the PM depends on the diameter of the glass spheres and the hydraulic diameter of the test section and is calculated from the equation below **(Salim, 2008):**

$$\varepsilon = \frac{V_c - V_P}{V_c} \quad (1)$$

$$V_c = A_c \text{ x } L \rightarrow H \text{ x } W \text{ x } L \quad (2)$$

$$V_p = \tfrac{4}{3}\pi r^3 n \quad (3)$$

where V_c is the volume of a channel containing PM (m^3), V_p is the volume of PM (m^3), A_c is the cross-section area of the channel (test section) (m^2), r is the radius of PM (glass spheres) (m), n is the number of a PM, and ε the porosity of PM.

For a channel at layer (20 mm of PM $\rightarrow n = 10854$), (40 mm of PM $\rightarrow n = 21708$), and (60 mm of PM $\rightarrow n = 32562$).

- **Thermal Conductivity and Density of PM**

The thermal conductivity (0.87 W/m^2) of the PM of the type of glass spheres was calculated based on a previous study by the researcher **(Hilal et al., 2012)**, and the density value of (2510 kg/m^3).

4. PROCEDURE OF EXPERIMENTAL WORK

After partially filling the channel (test section) with the PM (glass spheres), the following steps were taken to conduct the experiments:

- Controlling the blower's operation and airflow through the test section of a channel via valve and regulator.
- Turning on the electrical heater, the input power was changed to provide the necessary heat flux under the test section. Also, to create a steady-state situation, 120 minutes are needed.
- Record the inlet and outlet temperature of the working fluid (air) via a digital thermometer.
- Record the temperatures of the test section via thermocouples type (K).
- Record the average velocity of the fluid (Air) leaving the test section of a channel via a digital anemometer.
- Repeat the same steps above with a different velocity and a PM layer.

5. DATA PROCESSING

The following equations are used to analyze the forced convective heat transfer process of a channel partially filled with PM based on experimental data:

5.1 Air Bulk Temperature

The following relation may be used to compute the bulk air temperature **(Salim, 2008):**

$$T_b = \left(\frac{T_i + T_o}{2}\right) + 273.15 \quad (4)$$

where T_b is the bulb temperature (°C), T_i and T_o are a test section's inlet and outlet temperature, respectively (°C).

5.2 Properties of Working Fluid (air)

The relationship shown below may be used to derive the air qualities that verbally depend on the bulk temperature **(Salim, 2008):**

$$\rho_a = 4.93 - 0.026T_b + 6.4\times10^{-5}T_b^2 - 7.5\times10^{-8}T_b^3 + 3.36\times10^{-11}T_b^4 \quad (5)$$

$$\mu_a = 1.3\times10^{-6} + 5\times10^{-8}T_b + 1.2\times10^{-12}T_b^2 - 3.3\times10^{-13}T_b^3 + 12.6\times10^{-16}T_b^4 \quad (6)$$

$$k_a = 1.43\times10^{-16} + 9.3\times10^{-5}T_b + 3.4\times10^{-9}T_b^2 - 9.8\times10^{-11}T_b^3 + 8.4\times10^{-14}T_b^4 \quad (7)$$

$$\mathrm{Pr}_a = 0.79 - 1.1\times10^{-4}T_b - 1.35\times10^{-6}T_b^2 + 3.37\times10^{-9}T_b^3 + 2.2\times10^{-12}T_b^4 \quad (8)$$

$$Cp_a = 1.09 - 0.001T_b + 3.78\times10^{-6}T_b^2 - 6.27\times10^{-9}T_b^3 + 4.14\times10^{-12}T_b^4 \quad (9)$$

5.3 Average Velocity of Working Fluid (air)

The average air velocity exiting the test section was calculated using a typical digital anemometer device type (UT363S), as shown in **Fig. 6**. by taking nine readings of the test clip and finding the average for them such that:

$$u_a = \frac{u_1 + u_2 + u_3 + u_4 + u_5 + u_6 + u_7 + u_8 + u_9}{9} \quad (10)$$

Figure 6. Vane type of digital anemometer UT363S.

5.4 Mass Flow Rate

The air mass flow rate ($\dot{m}$) may be computed using the following equation **(Mahdi, 2021)**:

$$\dot{m} = \rho_a \times A_c \times u_a \quad (11)$$

where ρ_a is the density of working fluid (air) (kg/m^3), A_c is the cross-sectional area of the

channel (test section) (m^2), and u_a is the average velocity of working fluid (air) (m/s).

5.5 Convective Heating Transfer

It is possible to compute the convective heat transfer from the air **(Salim, 2008):**

$$Q = \dot{m} \times Cp_a \times (T_o - T_i) \quad (12)$$

$$\bar{q} = \frac{Q}{A_s} \quad (13)$$

where Q is the convection heat transfer (W), Cp_a is the specific heat at constant pressure (J/kg. °C), $\bar{q}$ is the heat flux (W/m^2), and A_s is the surface area of a channel (test section) (m^2).

5.6 Local Heat Transfer Coefficient

The following relation may be used to determine the local heat transfer coefficient **(AL-Thaher, 2000):**

$$h_z = \frac{\bar{q}}{\Delta t_z} \quad (14)$$

$$\Delta t_z = (T_s)_z - (T_b)_z \quad (15)$$

$$(T_b)_z = T_i + \frac{z}{L}(T_o - T_i) \quad (16)$$

where $(T_s)_z$ is the average temperature at two locations in the test section of a channel (°C).

5.7 Local Nusselt Number

The Nusselt number represents the ratio of convective heat transfer to conductive heat transfer (Nu_z) **(AL-Thaher, 2000)**. The following equation is used to calculate the local Nusselt number based on five thermocouple sites within the test section:

$$Nu_z = \frac{h_z D_h}{k_{eff}} \quad (17)$$

$$k_{eff} = \varepsilon k_a + (1-\varepsilon) k_s \quad (18)$$

where k_{eff} is effective thermal conductivity (W/m. °C), k_a is the thermal conductivity of the working fluid (air) (W/m. °C), ε is the porosity of PM (glass spheres), and k_s is the thermal conductivity of PM (glass spheres) (W/m. °C).

5.8 Overall Input Power

Calculate as follows to determine the total input power delivered to the channel **(Shehab, 2016):**

$$P_{in} = I \times V_o \quad (19)$$

where P_{in} is the input power to the channel (W), V_0 is the voltage supplied to the channel (volt), and I is the current supplied to the channel (A).

5.9 Losses Heat

The heat losses from the heated channel are calculated **(AL-Thaher, 2000):**

$$Q_{losses} = 1 - \frac{Q}{P_{in}} \quad (20)$$

5.10 Reynolds Number

The Reynolds number represents the ratio of the inertial force over the viscous force and can be calculated depending on the following equation **(Lafta and Mohammed, 2023):**

$$\mathrm{Re} = \frac{\rho_a u_a D_h}{\mu_a} \quad (21)$$

$$D_h = \frac{4 \times A_c}{Pe} \quad (22)$$

where ρ_a is the density of working fluid (air) (kg/m^3), u_a is the average velocity of working fluid (air) (m/s), D_h is the hydraulic diameter of a channel (m), and μ_a is the dynamic viscosity of working fluid (air) (Pa. s).

5.11 Particle Diameter-Based Reynolds Number

Reynolds number depends on particle diameter **(AL-Thaher, 2000)** and is evaluated as:

$$\mathrm{Re}_p = \frac{\rho_a u_a D_P}{\mu_a} \quad (23)$$

where D_p is the diameter of PM (m^2).

5.12 Modified Reynolds Number

The modified Reynolds number depends on particle diameter **(AL-Thaher, 2000)** and is calculated as follows:

$$\mathrm{Re}^* = \frac{\mathrm{Re}_P}{(1-\varepsilon)} \quad (24)$$

5.13 Average of Nusselt Number

The average Nusselt number represents the sum of the local Nusselt number within the test section **(AL-Thaher, 2000)** and can be calculated using the following equation**:**

$$Nu_{ave} = \frac{1}{L} \int_{x=0}^{x=L} Nu_z dz \quad (25)$$

By computing this integration with the help of the trapezoidal rule:

$$\int_0^L Nu_L dL = \frac{\Delta L}{2} [Nu_1 + 2Nu_2 + 2Nu_3 + \ldots\ldots + Nu_n] \quad (26)$$

where ΔL is the d*istance between two section* for a test section (m).

5.14 Pressure Drop and friction factor

The pressure difference ΔP across the test section is evaluated such that **(Sawhney, 2011):**

$$\Delta P = \rho_{water} \times g \times \Delta H \quad (27)$$

where g is the acceleration gravity (m/s^2), and ΔH is the difference height (m).

The friction factor f across the test section of a channel of length L can be calculated such that **(Adrian Bejan, 2013):**

$$f = \frac{\Delta P}{L} \frac{d_p}{\rho_a u_a^2} \frac{\varepsilon^3}{1-\varepsilon} \quad (28)$$

6. RESULTS AND DISCUSSION

6.1 Distribution of Temperatures

The temperature distribution for the PM layers along the channel (test section) (plain, 20, 40, and 60 mm) in layers is depicted in **Fig. 7.** depicts. The PM with a layer of (60 mm) and fluid velocity value of (0.75 m/s) had the largest temperature distribution. With an increase in the length for each layer of the PM, it can be noted that local surface temperatures of the test section increase. This is owing to the substantial heat increase brought on by the fluid's movement through the test section. In addition, the temperature distribution is altered by varying the layer of the PM in comparison to when the PM was not present in the channel. The fluid temperatures rise due to the blockage between the PM and the liquid flow.

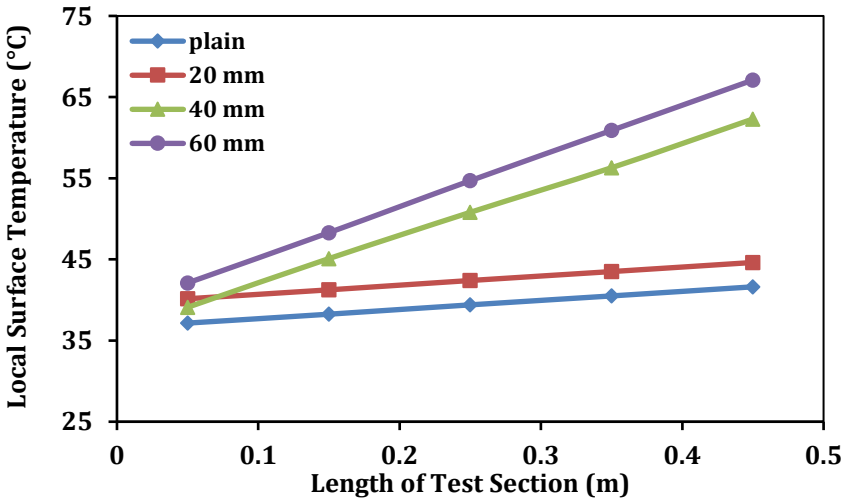

Figure 7. Temperature distribution for the PM layer thickness (plain, 20, 40, and 60 mm).

6.2 Local Heat Transfer Coefficient

Figs. 8 to 11 show the relationship between the local heat transfer coefficient and the test section length for the fluid flow direction in the channel for each Reynolds number.

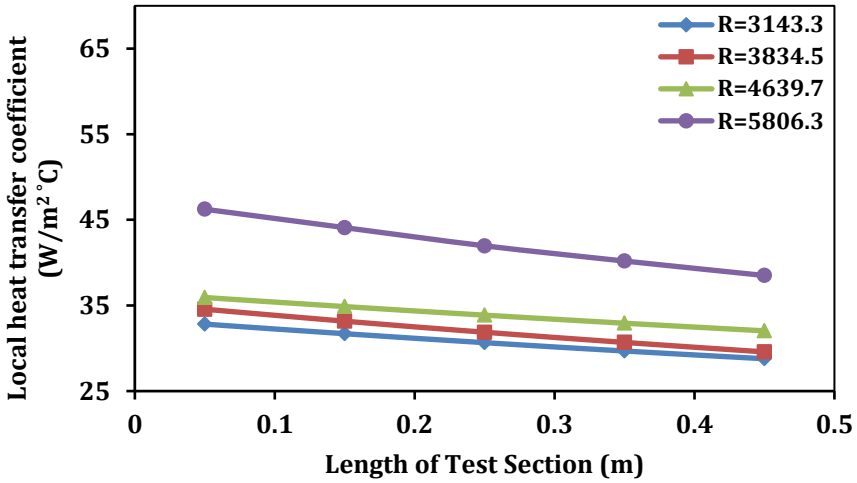

Figure 8. Local heat transfer coefficient vs length of test section for a plain channel at different Reynolds numbers.

The local heat transfer coefficient decreases progressively along the test section since the temperature difference between the fluid and wall widens as the Reynolds number rises.

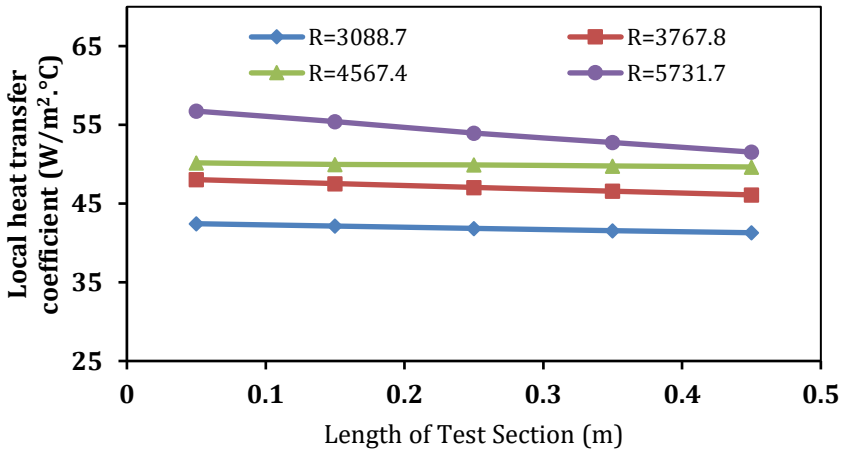

Figure 9. Local heat transfer coefficient along the test section for 20 mm PM layer for different Reynolds numbers.

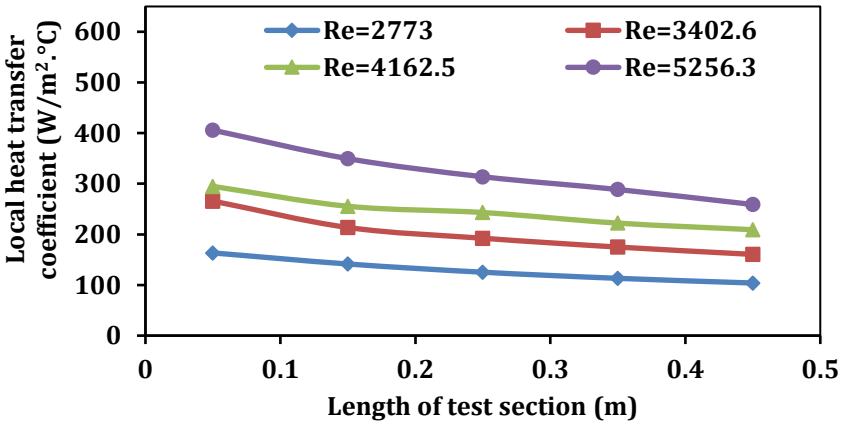

Figure 10. Local heat transfer coefficient along the test section for 40 mm PM layer for

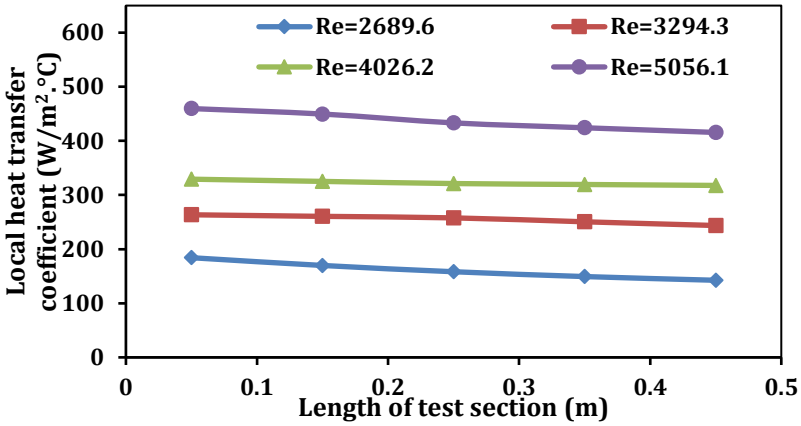

Figure 11. Local heat transfer coefficient along the test section for 60 mm PM layer for different Reynolds numbers.

6.3 Locally Nusselt Number

The relationship between the local Nusselt number and the length of the test section for the direction of fluid flow in the channel is shown in **Figs. 12 to 15.** It can be noted that a progressive decrease in the local Nusselt number with an increase in the length of the test section for each Reynolds number because the Nusselt number increases and decreases depending on the heat transfer coefficient.

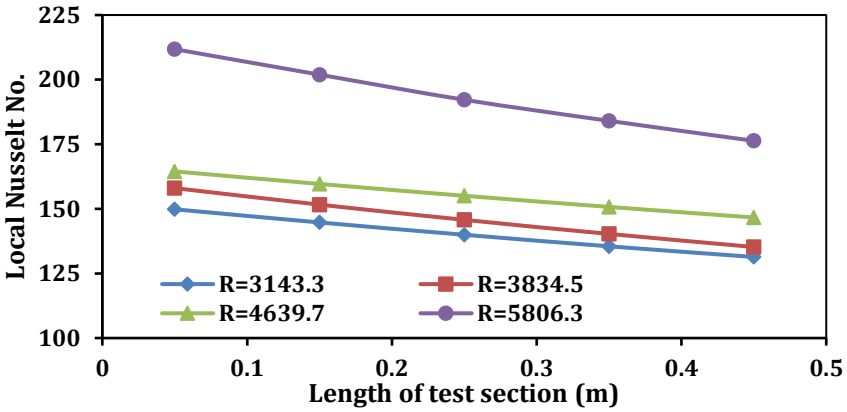

Figure 12. Local Nusselt number along the plain channel for different Reynolds numbers.

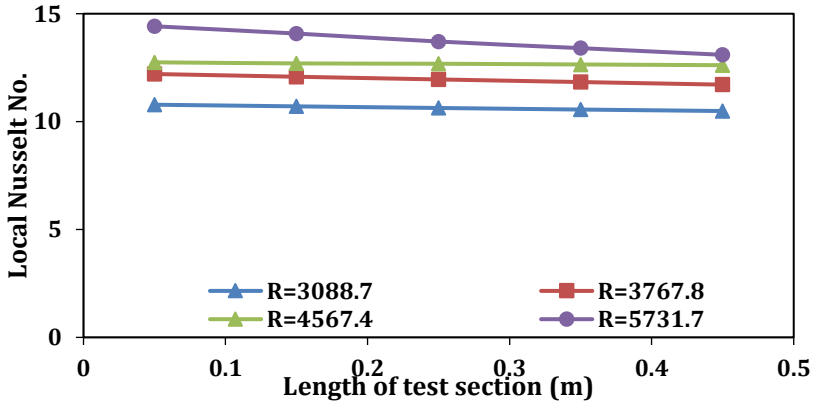

Figure 13. Local Nusselt number along the test section with (20 mm) PM layer for different

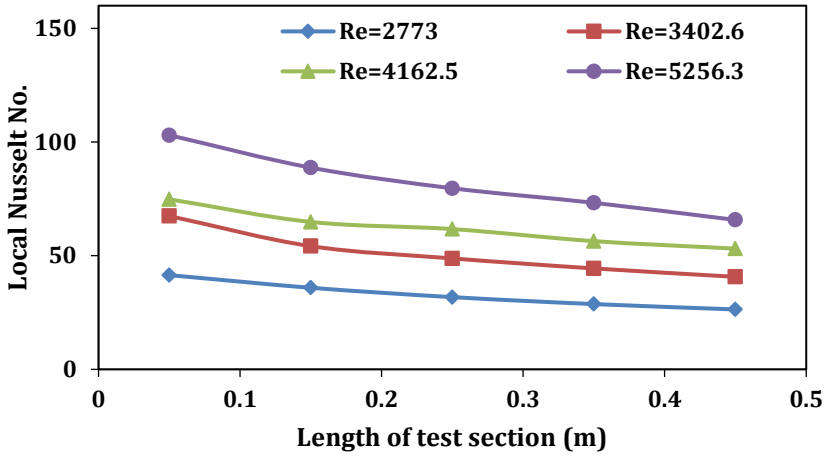

Figure 14. Local Nusselt number along the test section with (40 mm) PM layer for different Reynolds numbers.

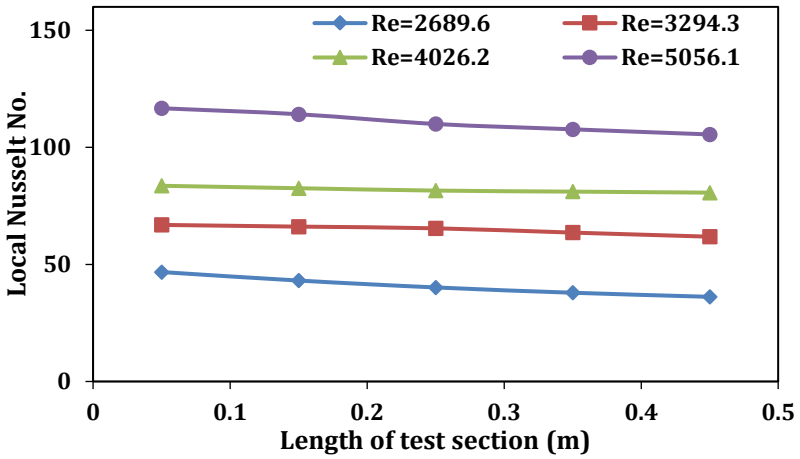

Figure 15. Local Nusselt No. along the test section with (60 mm) PM layer for different Reynolds No.

6.4 Average of Heat Transfer Coefficient

Fig. 16. shows the average heat transfer coefficient with the Reynolds number at each PM layer (plain, 20, 40, and 60 mm), respectively. It can be seen that the average heat transfer coefficient increased gradually by increasing the Reynolds number and also by increasing the thickness of the porous medium layer. The highest value appeared at (60 mm). Also, at the maximum Reynolds number, the percentage enhancement of the average heat transfer coefficient for each layer is (22.025, 86.86, and 90.335%) respectively.

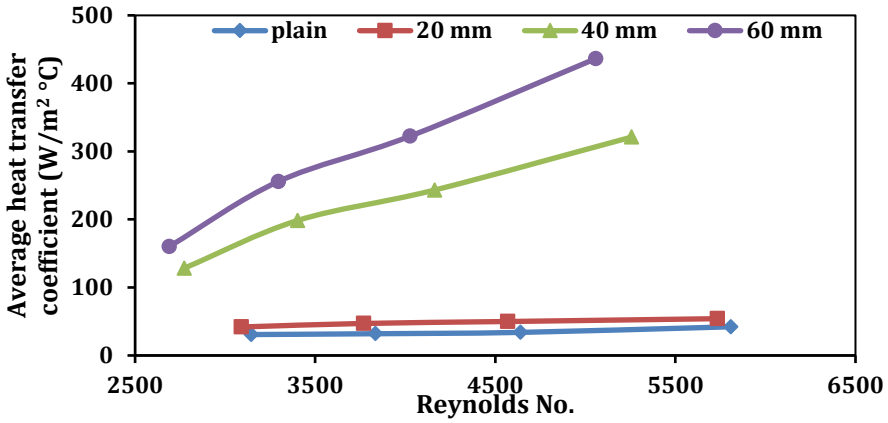

Figure 16. Average heat transfer coefficient vs. Reynolds No. for different PM layer thickness.

6.5 Average of Nusselt Number

With Reynolds numbers ranging from (2689.6 to 5806.3) and a constant heat flow (4791.7 W/m^2), **Fig. 17.** shows the average Nusselt number with Reynolds number in a channel at different layers of PM (plain, 20, 40, and 60 mm). It can be noted that the average Nusselt number increases progressively with the increase in the Reynolds number, and the highest value appeared at the height of the plain channel because it depends on the thermal conductivity of the fluid compared to the absence of the PM, which depends on the effective thermal conductivity.

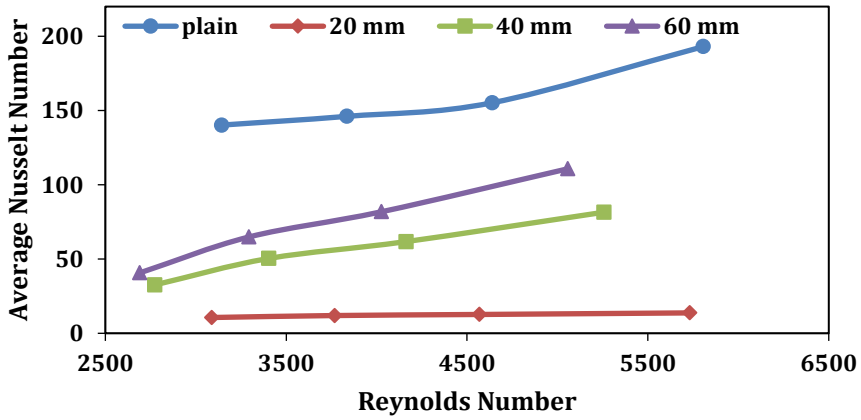

Figure 17. Average Nusselt number vs Reynolds number for a test section at different layers of PM.

6.6 Pressure Drop and Friction Factor

Figures 18 and **19** show an increase in the pressure difference and a decrease in the friction factor with Reynolds number, respectively, at the layer of PM (60 mm). It can be seen that the pressure difference increases gradually with an increase in the Reynolds number, and the friction factor decreases gradually with an increase in the Reynolds number because the amount of velocity is inversely proportional to the friction factor.

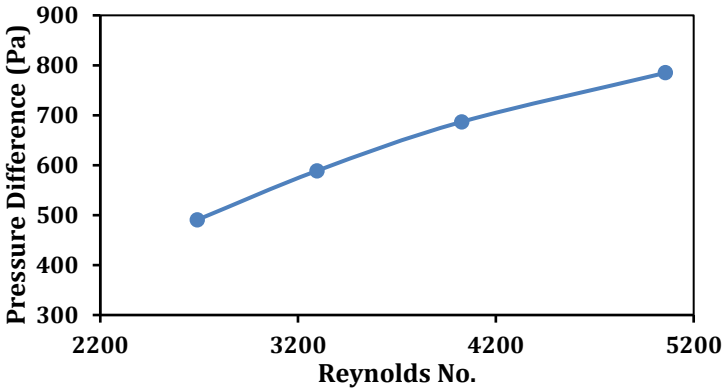

Figure 18. Pressure difference against Reynolds number at thickness PM layer (60 mm).

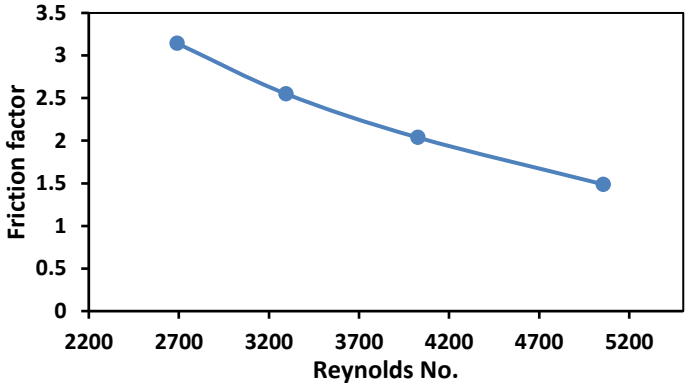

Figure 19. Friction factor against Reynolds number at thickness PM layer (60 mm).

7. COMPARISON WITH PREVIOUS WORK

Figure 20. compares the variation of fluid's temperature along the channel's test section for the current work with that for **(Youssif et al., 2020)** considering the specification given in **Table 1.** The results showed that the same behavior in increase of the local temperatures with the test section length is reported.

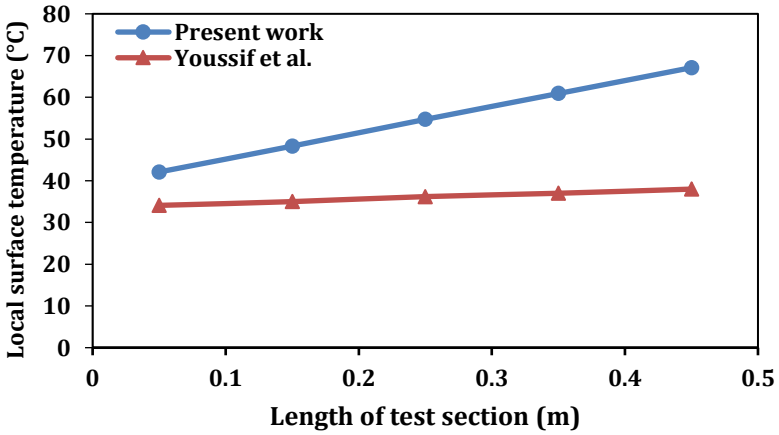

Figure 20. Local surface temperature vs length of test section for present work with previous work **(Youssif et al., 2020)**.

Table 1. Properties of comparison process for present study with previous work **(Youssif et al., 2020)**.

Work	Working Fluid	Reynolds Number	Type of PM
Present	Air	2689.6 to 5806.3	Glass Spheres
(Youssif et al., 2020)	Water	500 to 1500	Steel Spheres

8. CONCLUSIONS

Study of forced convection heat transfer due to the presence of an electric blower initially connected to a channel of square cross-section (120 x 120 mm^2) partially filled with glass balls used as a PM. The lower of the test section is exposed to a constant and uniform heat flux (4791.7 W/m^2) along the fluid (air) flow axis, while the other walls are thermally insulated to avoid losses. The most important conclusions of the current study include the following points:

- The surface temperature distribution of the fluid for each layer of the PM (plain, 20, 40, and 60 mm) decreases with increasing Reynolds number.
- The local heat transfer coefficient and local Nusselt number decrease with the increasing length of the test section when the fluid flows for each PM layer.
- The temperature distribution increases with the test section's length when the fluid is flowing.
- The average Nusselt number increases with the Reynolds number increase.
- The height of the PM at layer (60 mm) had the highest improvement for the average heat transfer coefficient by (90.335%), while the other layers (20 and 40 mm) gave an improvement percentage of (22.025 % and 86.867 %), respectively.
- The gap in the local heat transfer coefficient readings and the local Nusselt number in the **Figs. 8, 12, and 13** occurred due to increasing the fluid velocity and temperature at the PM layer (60 mm) compared to the other layers.
- The pressure difference across the test section increases gradually when the value of the Reynolds number increases.
- The friction factor decreases gradually with increasing the velocity of the fluid passing through the test section.
- The value of the average Nusselt number for the plain channel increases when calculated because it depends on the thermal conductivity of the fluid (air) compared to the average Nusselt number for the channel partially filled with PM, which depends on the effective thermal conductivity.

NOMENCLATURE

Symbol	Description	Symbol	Description
A_C	Cross section area, m^2	PM	Porous media.
A_s	Surface area, m^2	P_{in}	Input power, W
Cp	Specific heat at constant pressure, kj/kg.K	Pr	Prandtl number.
D_h	Hydraulic diameter, m	Q	Convection heat transfer, W
D_p	Porous media diameter, m	r	Radius of porous media, m
f	Friction factor, dimensionless.	Re	Reynolds number.
g	Gravitional acceleration, m/s^2	T_b	Bulk temperature, °C

H	Height of channel, m	T_i	Inlet temperature, °C
I	Current supplied, A	T_o	Outlet temperature, °C
k_{eff}	Effective thermal conductivity, W/m.°C	T_s	Surface temperature, °C
k_a	Air thermal conductivity, W/m.°C	u_a	Air velocity, m/s
L	Length of test section, m	W	Width of channel, m
$\dot{m}$	Mass flow rate, kg/s	Δ	Difference, dimensionless.
n	Number of balls , dimensionless.	ε	Porosity, dimensionless.
Nu	Nusselt number, dimensionless.	μ	Dynamic viscosity, Pa.s
Pe	Perimeter, m	ρ	Density, kg/m^3

Acknowledgements

This work was supported by the University of Babylon, College of Engineering Al Musaib, Automoblies Engineering Department (Grant Nos.2501).

Credit Authorship Contribution Statement

Sarmad A. Ali: Writing – original draft, Investigation, Validation, Software, Methodology. Suhad A. Rasheed: Writing – review & editing, Data curation, Analysis of results.

Declaration of Competing Interest

The authors declare that they have no known competing financial interests or personal relationships that could have appeared to influence the work reported in this paper.

REFERENCES

Abood, F.A., 2011. Numerical study of laminar free convection heat transfer inside porous media-filled triangular enclosure. *Basrah Journal for Engineering Sciences*, 11(1), pp. 44-56.

Adrian Bejan, 2013. *Convection heat transfer*, John Wiley & Sons, Inc., Canada, 4th ed., pp. 428-477.

Ali, L.F., 2015. Natural and mixed convection in square vented enclosure filled with metal foam. *Journal of Engineering*, 21(11), pp. 60-79. Doi:10.31026/j.eng.2015.11.04

AL-Thaher, M.A., 2000. Mixed convection heat transfer in a horizontal tube filled with porous media, Ph.D. Thesis, *University of Technology*, Baghdad.

Antonio, B., Eugenia R., and Leiv S., 2013. Convective instability in a horizontal porous channel with permeable and conducting side boundaries. *Springer Science and Business Media Dordrecht*, 99 (3), pp. 515-533. Doi:10.1007/s11242-013-0198-y

Baragh, S., Shokouhmand, H. and Ajarostaghi, S.S.M., 2019. Experiments on mist flow and heat transfer in a tube fitted with porous media. *International Journal of Thermal Sciences*, 137, pp. 388-398. Doi:10.1016/j.ijthermalsci.2018.11.030

Dawood, A.S., and Hmood, O.B., 2006. Through porous medium enclosing a rectangular isothermal body. *Al- Rafidain Engineering*, 14 (1), pp. 73-86. Doi:10.33899/rengj.2006.46273

Guo, C., Li, Y., Nian, X., Xu, M., Liu, H. and Wang, Y., 2020. Experimental study on the slip velocity of turbulent flow over and within porous media. *Physics of Fluids*, 32(1), pp. 1-14. Doi:10.1063/1.5128479

Hilal, K.H., Fadhl, L.T. and Faraj, S.N., 2012. Experimental investigation of heat transfer and pressure drop in square metal packed duct with different boundary heating. *Engineering and Technology*

Journal, 30(6), pp. 1082-1107. Doi:10.30684/etj.30.6.13

Hilal, K.H., Saleh, A.M. and Ebraheem, M.H., 2014. An experimental study on heat transfer enhancement for porous heat exchange in rectangular duct. *Engineering and Technology Journal*, *32*(11), pp. 2788-2802. Doi:10.30684/etj.32.11A.15

Kemerli, U. and Kahveci, K., 2018. Local thermal non-equilibrium modelling of convective heat transfer in high porosity metal foams. *WIT Transactions on Engineering Sciences*, 120, pp. 293-301. Doi:10.2495/AFM180301

Khadhrawi, S., Oueslati, F.S. and Bennacer, R., 2020. Mixed convection in a channel partially filled with metal foam blocks. In MATEC Web of Conferences (Vol. 330, p. 01044). EDP Sciences. Doi:10.1051/matecconf/202033001044

Kurtbas, I. and Celik, N., 2009. Experimental investigation of forced and mixed convection heat transfer in a foam-filled horizontal rectangular channel. *International journal of heat and mass transfer*, 52(5-6), pp. 1313-1325. Doi:10.1016/j.ijheatmasstransfer.2008.07.050

Lafta, H.D. and Mohammed, D.O., 2023. Experimental investigation of heat transfer enhancement in a double pipe heat exchanger using compound technique of transverse vibration and inclination angle. *Journal of Engineering*, 29(5), pp. 90-105. Doi:10.31026/j.eng.2023.05.07

Li, P., Zhang, J., Wang, K. and Xu, Z., 2019. Heat transfer characteristics of thermally developing forced convection in a porous circular tube with asymmetric entrance temperature under LTNE condition. Applied Thermal Engineering, 154, pp. 326-331. Doi:10.1016/j.applthermaleng.2019.03.109

Li, Q. and Hu, P., 2019. Analytical solutions of fluid flow and heat transfer in a partial porous channel with stress jump and continuity interface conditions using LTNE model. *International Journal of Heat and Mass Transfer*, 128, pp. 1280-1295. Doi:10.1016/j.ijheatmasstransfer.2018.08.132

Majel, B.M. and Obaid, Z.A.H., 2024. Experimental investigation of forced convective heat transfer and fluid flow in a mini heat pipe with rectangular micro grooves. *Journal of Thermal Engineering*, 10(1), pp.207-218. Doi:10.18186/thermal.1429961

Mahdi, A.N., Hasan, M.R. and Rasheed, S.A., 2021. Experimental study of forced convection heat transfer through porous media inside a rectangular duct of fully developed region, *In IOP Conference Series: Materials Science and Engineering*, 1076 (1), P. 012073. Doi:10.1088/1757-899X/ 1076/ 1/ 012073

Makkawi, Y. T., 1995. Investigation of heat transfer in a rectangular packed duct with constant heat flux and symmetrical wall temperatures, M.Sc. Thesis, King Fahd University of Petroleum & Minerals.

Moghadasi, H., Aminian, E., Saffari, H., Mahjoorghani, M. and Emamifar, A., 2020. Numerical analysis on laminar forced convection improvement of hybrid nanofluid within a U-bend pipe in porous media. *International Journal of Mechanical Sciences*, 179, P. 105659. Doi:10.1016/j.ijmecsci.2020.105659

Mohammed, A.A., 2020. Review on heat transfer process inside open and closed porous cavity. *Journal of Engineering*, 26(9), pp. 204-216. Doi:10.31026/j.eng.2020.09.14

Nazari, S. and Toghraie, D., 2017. Numerical simulation of heat transfer and fluid flow of Water-CuO Nanofluid in a sinusoidal channel with a porous medium. *Physica E: Low-dimensional Systems and Nanostructures*, 87, pp. 134-140. Doi:10.1016/j.physe.2016.11.035

Nimvari, M.E., Maerefat, M. and El-Hossaini, M.K., 2012. Numerical simulation of turbulent flow and heat transfer in a channel partially filled with a porous media. *International Journal of Thermal Sciences*, 60, pp. 131-141. Doi:10.1016/j.ijthermalsci.2012.05.016

Pastore, N., Cherubini, C., Rapti, D. and Giasi, C.I., 2018. Experimental study of forced convection heat

transport in porous media. *Nonlinear Processes in Geophysics*, 25(2), pp. 279-290. Doi: 10.5194/npg-25-279-2018

Poulikakos, D., and Renken, K., 1987. Forced convection in a channel filled with porous medium including the effects of flow inertia variable porosity and Brinkman friction. *ASME Journal of Heat Transfer,* 109 (4), pp. 880-888. Doi:10.1115/1.3248198

Rasheed, S.A. and Abood, J.M., 2017. Force convection heat transfer from a different cross section cylinder embedded in porous media. *Al-Nahrain Journal for Engineering Sciences*, 20(3), pp. 727-736. Doi:10.13140/RG.2.2.14800.25600

Salim, T.K., 2008. An experimental study for heat transfer enhancement by laminar forced convection from horizontal and inclined tube heated with constant heat flux, using two types of porous media. *Tikrit Journal of Engineering Sciences*, 15(2), pp. 15-36. Doi:10.25130/tjes.15.2.09

Sawhney, G. S., 2011. *Fundamentals of fluid mechanics*, I. K. International Pvt Ltd, 2nd ed., pp.66.

Seki, N., Fukusako, S. and Inaba, H., 1978. Heat transfer in a confined rectangular cavity packed with porous media. *International Journal of Heat and Mass Transfer*, *21*(7), pp. 985-989. Doi:10.1016/0017-9310(78)90190-4

Shehab, S.N., 2016. Experimental investigation of natural convection into a horizontal annular tube with porous medium effects. *Journal of Engineering*, 22(12), pp. 103-117. Doi:10.31026/j.eng.2016.12.07

Shokouhmand, H., Jam, F. and Salimpour, M.R., 2011. The effect of porous insert position on the enhanced heat transfer in partially filled channels. *International Communications in Heat and Mass Transfer*, 38(8), pp. 1162-1167. Doi:10.1016/j.icheatmasstransfer.2011.04.027

Torabi, M., Zhang, K., Yang, G., Wang, J. and Wu, P., 2015. Heat transfer and entropy generation analyses in a channel partially filled with porous media using local thermal non-equilibrium model. *Energy*, 82, pp. 922-938. Doi:10.1016/j.energy.2015.01.102

Varol, Y., Oztop, H.F., Mobedi, M. and Pop, I., 2008. Visualization of natural convection heat transport using heatline method in porous non-isothermally heated triangular cavity. *International Journal of Heat and Mass Transfer*, 51(21-22), pp. 5040-5051. Doi:10.1016/j.ijheatmasstransfer.2008.04.023

Youssif, Y.F., Kadhum, M.H. and Ali, A.H., 2020, November. Experimental study for laminar forced convection heat transfer enhancement from horizontal tube heated with constant heat flux, by using different types of porous media. *In IOP Conference Series: Materials Science and Engineering,* 928 (2), IOP Publishing. Doi:10.1088/1757-899X/928/2/022086

Zhu, X., Pan, D., Gao, Y., Guo, Y., Guan, Y. and Ma, H., 2023. Heat transfer enhancement in a regenerative cooling channel using porous media. *Chemical Engineering and Processing-Process Intensification*, 183, P.109234. Doi:10.1016/j.cep.2022.109234